Anal. Chem. **2010,** *82,* 1858–1866

Fluorescent Carrier Ampholytes Assay for Portable, Label-Free Detection of Chemical Toxins in Tap Water

M. Bercovici,[†] G. V. Kaigala,[‡] C. J. Backhouse,[§] and J. G. Santiago*,[‡]

Department of Aeronautics and Astronautics, Stanford University, Stanford, California 94305, Department of Mechanical Engineering, Stanford University, Stanford, California 94305, and Department of Electrical and Computer Engineering, University of Alberta, Edmonton Alberta T6G 2V4, Canada

We present a novel method for fluorescence-based indirect detection of analytes and demonstrate its use for label-free detection of chemical toxins in a hand-held device. We fluorescently label a mixture of low-concentration carrier ampholytes and introduce it into an isotachophoresis (ITP) separation. The carrier ampholytes provide a large number of fluorescent species with a wide range of closely spaced effective electrophoretic mobilities. Analytes focus under ITP and displace subsets of these carrier ampholytes. The analytes are detected indirectly and quantified by analyzing the gaps in the fluorescent ampholyte signal. The large number (on the order of 1000) of carrier ampholytes enables detection of a wide range of analytes, requiring little *a priori* knowledge of their electrophoretic properties. We discuss the principles of the technique and demonstrate its use in the detection of various analytes using a standard microscope system. We then present the integration of the technique into a self-contained hand-held device and demonstrate detection of chemical toxins (2-nitrophenol and 2,4,6-trichlorophenol) in tap water, with no sample preparation steps.

Environmental monitoring efforts, and water quality assessment in particular, would benefit from widely available and inexpensive chemical assays and sensor technologies.[1] Gas and liquid chromatography methods, and their coupling to mass spectrometry, currently are standard methods suggested by the United States Environmental Protection Agency (EPA) for the detection of chemical toxins in drinking water.[2] While these methods are considered sufficiently sensitive and accurate, their use is mostly confined to laboratory settings, because of their size, weight, power requirement, peripheral equipment, cost, and sample preparation steps.[3] There is a need for detection techniques that are cost-effective, sensitive, and portable.

One approach toward widespread toxin detection is the miniaturization of traditional chromatography systems. Although there have been efforts to reduce size and weight significantly,[4] scaling down and integrating the essential system components remains a challenge. Much of the work is focused on implementation of an efficient stationary phase in microstructures, and in miniaturization of pressure sources, pumps, and valves.[5]

An alternative approach to realizing low-cost and portable toxins detection is developing novel assays that have increased functionality, avoid complex sample preparation (e.g., labeling), and are compatible with inexpensive system architectures. Fluorescence-based detection is the most sensitive method for on-chip applications,[6] but this methodology typically requires autofluorescent analytes (a property that is not possessed by most toxins of interest) or fluorescent labeling (e.g., using immunoassays[7]). Kuhr and Yeung[8] demonstrated indirect detection through displacement of fluorescence-detectable background ions in capillary electrophoresis (CE). However, high analyte concentrations were required for the displacement physics, limiting sensitivity to analyte concentrations of $\sim$100 μM.

Recently, several fluorescence-based indirect detection methods based on isotachophoresis (ITP) have been proposed.[9,10] In ITP, sample ions simultaneously focus and separate according to their electrophoretic mobilities between a leading electrolyte (LE) and trailing electrolytes (TE). This creates purified, high-concentration, adjacent zones electromigrating at a uniform velocity. Chambers and Santiago[9] developed an indirect detection method called nonfocusing, wherein sample zones are detected by analyzing the local intensity of a nonfocusing fluorescent tracer molecule as it electromigrates through ITP zones of unlabeled analytes. The NFT method requires only a single fluorophore for multiple analytes, but the fluorescence signal strength is on the order of the initial concentration (which can be limited by self-quenching, wall adsorbance, or interaction with analytes). Khurana and Santiago[10] presented an indirect detection ITP assay that uses mobility markers to identify and quantify unlabeled analytes. The

* Author to whom correspondence should be addressed. Fax: (650) 723-7657. E-mail: juan.santiago@stanford.edu.

† Department of Aeronautics and Astronautics, Stanford University.

‡ Department of Mechanical Engineering, Stanford University.

§ Department of Electrical and Computer Engineering, University of Alberta.

(1) Wanekaya, A. K.; Chen, W.; Mulchandani, A. *J. Environ. Monit.* **2008**, *10*, 703–712.

(2) Safe Drinking Water Act Analytical Methods and Laboratory Certification, U.S. Environmental Protection Agency, http://www.epa.gov/safewater/methods/analyticalmethods.html.

(3) Janasek, D.; Franzke, J.; Manz, A. *Nature* **2006**, *442*, 374–380.

(4) Lindner, D. *Lab Chip* **2001**, *1*, 15N–19N.

(5) Mello, A. D. *Lab Chip* **2002**, *2*, 48N–54N.

(6) Landers, J. P. *Handbook of Capillary and Microchip Electrophoresis and Associated Microtechniques*, CRC Press; Boca Raton, FL, 2007.

(7) Jiang, X.; Li, D.; Xu, X.; Ying, Y.; Li, Y.; Ye, Z.; Wang, J. *Biosens. Bioelectron.* **2008**, *23*, 1577–1587.

(8) Kuhr, W. G.; Yeung, E. S. *Anal. Chem.* **1988**, *60*, 2642–2646.

(9) Chambers, R. D.; Santiago, J. G. *Anal. Chem.* **2009**, *81*, 3022–3028.

(10) Khurana, T. K.; Santiago, J. G. *Anal. Chem.* **2008**, *80*, 279–286.

10.1021/ac902526g
Published on Web 02/08/2010

approach mixes analytes with carefully selected fluorescent species (termed mobility markers) that focus into ITP zones, along with analytes. Gaps in the fluorescence signal of the fluorescent markers then indicate the presence and quantity of the specific analytes which they bracket. The strong ion displacement physics of ITP resulted in the ability to detect ~10 μM nonfluorescent analytes while directly detecting fluorescent markers present at a concentration on the order of ~1 mM. Typically, analytes focus in peak mode (narrow, Gaussian-like shapes associated with low concentration) and, therefore, are easily identified using standard peak analysis. A disadvantage of the mobility markers technique is that marker molecules and ITP buffer conditions must be specifically selected for each analyte; in addition, there are typically only a limited number of available fluorophores with relevant mobilities. Despite these developments in indirect detection, there remains a need for a widely applicable, indirect fluorescence assay that can both detect a large number of analytes and is amenable to implementation in a low-cost device.

Portable devices with on-chip separation and fluorescence detection have been demonstrated. In early work, Burns et al.[11] demonstrated the integration of microelectronics with microfluidics. They demonstrated DNA analysis based on the integration of a photodiode and optical electronics, albeit with a substantial external infrastructure. They noted high-voltage functionality as the limiting factor in realizing a self-contained system. Lagally et al.[12] presented a portable system for fluorescence-based genetic analysis. They showed a limit of detection of 2−3 bacterial cells, but the technology relied on high-cost components such as confocal optics and a photomultiplier tube. Recent work by Behnam et al. presented a microelectronic chip capable of supplying, switching, and controlling high-voltage (hundreds of volts) from a 5 V source.[13] Based on this chip, Kaigala et al.[14] demonstrated CE on a relatively low-cost hand-held electrophoresis device with fluorescence detection. In a recent work, we presented an improved version of the device and demonstrated its use with isotachophoresis.[15]

The goal of the current work is the development of an indirect detection assay for toxin detection in tap water, which minimizes sample preparation and *ad hoc* assay design, and yet is also compatible with the handheld device.[15] We propose a new fluorescence-based indirect detection technique that leverages ITP and a mixture of a large number (on the order of 1000) of fluorescently labeled carrier ampholytes (CAs) as mobility markers. We mix analytes with fluorescently labeled CAs and segregate and focus the mixture using ITP. Each analyte can be detected and quantified as one of many possible gaps in the fluorescent CA signal. In contrast to the mobility marker implementation of Khurana and Santiago,[10] the current method does not require *a priori* choice of fluorophores and can be readily applied (without extensive and specific design) to a wide range of analytes. We discuss the principles of the method and demonstrate its use for the detection of several ideal analyte molecules. We present first experimental results using a microscope-based system; and demonstrate the detection of 2-nitrophenol (2NP) and 2,4,6-trichlorophenol (TCP) in tap water, without prior preparation steps. These are products and intermediates of industrial processes (e.g., production of plastics, drugs, herbicides) and common water pollutants,[16] and are classified as priority pollutants by the EPA.[16,17] We then demonstrate the detection of these toxins using our handheld, USB-powered electrophoresis device.

FLUORESCENT CARRIER AMPHOLYTES ASSAY

Carrier ampholytes (CAs) are mixtures of amphoteric species, typically artificially synthesized polypeptides. They are typically used in isoelectric focusing (IEF) to produce a stationary pH gradient.[18] Commercially available CAs contain between a few hundred to a few thousand different amphoteric species (more exact estimates are typically proprietary information), which possess a range of isoelectric points (pIs).[19] In IEF, a channel or gel separation column is filled with an ampholyte mixture. Under an applied electric field, ampholytes electromigrate, focus, and self-segregate to their respective pI, resulting in (an approximately linear) pH gradient. Amphoteric analytes introduced into this mixture electromigrate through the established pH gradient, separate, and focus at locations corresponding to their respective pI values. High concentrations of (nonfluorescent) CAs have been previously used with ITP to create a range of spacers between directly detectable analytes.[20,21] These traditional applications of CAs are in sharp contrast to their use in the assay we propose here. In this work, we use a low concentration of CAs to create a mixture of fluorescently labeled species with a large distribution of pK_a values. Using these labeled CAs in an environment whose pH is set primarily by the LE buffer (as is typical in ITP), we obtain species with a large distribution of finite (nonzero) effective electrophoretic mobilities.

Fluorescently labeled CAs have been used to locate ITP interfaces in a gel, but not in free solution and not for the purpose of specifically identifying sample species via analysis of the fluorescent signal. Schafer-Nielsen et al.[22] performed ITP analysis of human serum proteins with standard (nonfluorescent) molecular spacers to improve resolution. They added to the mixture fluorescently labeled CA which focused at the boundaries of these spacers, in locations where they also expected their macromolecules to focus. They therefore used labeled CAs to identify the (co-located) focusing sites of their analytes; and this made the process of cutting zones out of the gel for sample extraction easier. Fluorescamine-tagged CAs (they used ampholine, LKB, Sweden) were visualized using UV illumination. Here, we leverage and

(11) Burns, M. A.; Johnson, B. N.; Brahmasandra, S. N.; Handique, K.; Webster, J. R.; Krishnan, M.; Sammarco, T. S.; Man, P. M.; Jones, D.; Heldsinger, D.; Mastrangelo, C. H.; Burke, D. T. *Science* **1998**, *282*, 484–487.

(12) Lagally, E. T.; Scherer, J. R.; Blazej, R. G.; Toriello, N. M.; Diep, B. A.; Ramchandani, M.; Sensabaugh, G. F.; Riley, L. W.; Mathies, R. A. *Anal. Biochem.* **1998**, *257*, 95–100.

(13) Behnam, M.; Kaigala, G. V.; Khorasani, M.; Marshall, P.; Backhouse, C. J.; Elliott, D. G. *Lab Chip* **2008**, *8*, 1524–1529.

(14) Kaigala, G.; Behnam, M.; Bliss, C.; Khorasani, M.; Ho, S.; McMullin, J.; Elliott, D.; Backhouse, C. *IET Nanobiotechnol.* **2009**, *3*, 1–7.

(15) Kaigala, G. V.; Bercovici, M.; Behnam, M.; Elliott, D. G.; Santiago, J. G.; Backhouse, C. J. Manuscript in preparation, 2009.

(16) Baldwin, D.; Debowski, J. *Chromatographia* **1988**, *26*, 186–190.

(17) Jinadasa, K.; Mun, C. H.; Aziz, M. A.; Ng, W. J. *Water Sci. Technol.* **2004**, *50*, 119–124.

(18) Righetti, P. G. *Isoelectric Focusing*; Elsevier: Amsterdam, 1983.

(19) Righetti, P. G.; Simo, C.; Sebastiano, R.; Citterio, A. *Electrophoresis* **2007**, *28*, 3799–3810.

(20) Acevedo, F. *J. Chromatogr., A* **1989**, *470*, 407–414.

(21) Inano, K.; Tezuka, S.; Miida, T.; Okada, M. *Ann. Clin. Biochem.* **2000**, *37*, 708.

(22) Schafer-Nielsen, C.; Svendsen, P.; Rose, C. *J. Biochem. Biophys. Methods* **1980**, *3*, 97–128.

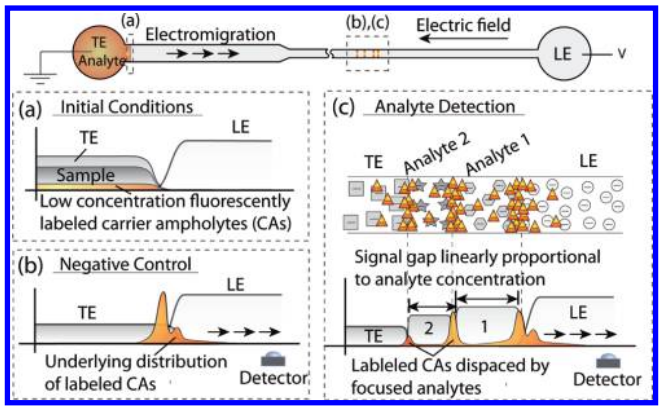

Figure 1. Schematic of isotachophoretic separation and indirect detection using the fluorescent carrier ampholytes assay. (a) A single microchannel is connected to two reservoirs and is initially filled with a leading electrolyte (LE). Sample is introduced along with prelabeled carrier ampholytes (CAs) into the trailing electrolyte reservoir. An electric field is applied along the channel. (b) In the absence of analytes (negative control), labeled CAs focus at a single interface between the LE and TE. This constitutes the baseline signal. (c) Analytes mixed with the TE separate into distinct, focused zones. Groups of fluorescent CAs are displaced by the analytes and analyte ions are identified as gaps or "valleys" in the fluorescent CA signal. For a fixed detection site, the gap width is proportional to the initial analyte concentration.

extend this idea of carrier−ampholyte fractionation to create a quantitative assay for indirect detection and identification of chemical species in on-chip ITP analysis.

In contrast to IEF, ITP uses leading electrolytes (LEs) and trailing electrolytes (TEs) to buffer and determine system pH with a relatively narrow range (often a pH difference of 1 pH unit or less between LE and TE). Under these conditions, a mixture of CAs introduced into the system can be regarded as a mixture of species with a large distribution of effective mobilities, determined by the relative difference between each pK_a and local pH. Many available CAs contain one or more primary amine groups, which makes them suitable for labeling with amine reactive dyes.[23] We use such labeling to create a large collection of fluorescent species with a wide range of closely spaced effective mobilities.

Figure 1 shows the principles of the technique schematically. We fill a channel and one of the end-channel reservoirs with LE. As we will discuss further below, the channel consists of two sections of different widths to improve assay sensitivity. We fill the other reservoirs with a mixture containing the TEs, sample, and a low concentration of labeled CAs. In the absence of analyte ions, the application of an electric field causes a subset of CAs to focus into a contiguous zone of fluorescence (the negative control) between the LE and TE. When analyte ions are mixed with the TEs, they also focus between LEs and TEs and thereby displace groups of fluorescent CAs. Analyte zones are detectable indirectly as "gaps" in the fluorescent signal. The basic physics are the same as those of the mobility marker assay of Khurana and Santiago;[10] but, here, the use of a large number of labeled CAs as markers yields unprecedented resolution and dynamic range. Multiple analyte detection is accomplished via ITP separation physics with a single fluorescence emission wavelength. We term the technique fluorescent carrier ampholytes (FCA) assay.

The use of a large number of FCAs as markers implies that very little *a priori* knowledge of analyte ion mobility is required for a wide range of analytes. Analytes should focus between LEs and TEs and have an effective mobility also bracketed by the very large range of CA mobilities. The large number of FCAs also implies a high dynamic range of identifiable analyte mobilities. A fluorescence zone will appear between any two analytes zones, provided that some subgroup of CAs possesses effective mobilities bracketed by the two analytes. The main limitation of the technique is that it is unable to detect analytes whose effective mobilities are higher than those of all the CAs (e.g., in anionic ITP, strongly ionized acids can have relatively high mobility). For weak electrolyte analytes, it is typically possible to design the pH of the system (by specifying the LE buffer) to achieve an effective mobility within the range of FCA mobilities.

THEORY

For low analyte concentrations and short times, the analyte in FCA assay is in "peak mode",[24] where it contributes negligibly to local conductivity. For increasing focused analyte concentrations, the analyte contributes more significantly to the local conductivity and eventually displaces CAs, effecting a noticeable change in the fluorescent signal. The limit of detection (LoD) of our assay can be described as the minimum analyte concentration for which a local decrease in the baseline CA signal can be detected (versus noise and run-to-run variations). In practice, minimizing the LoD is equivalent to maximizing the width of the plateau-mode[10] analyte zone width for a given initial analyte concentration. The dependence of the focusing rate and length of the analyte zone on the chemistry of the ITP buffers and applied current has been studied.[10,24] Everaerts et al.[25,26] first proposed the concept of "column coupling" as a method for increasing sample loading in ITP. In this method, a large inner diameter (ID) capillary is used to load a large volume of sample, which, in the next step, is separated and detected in a small-ID capillary. In this section, we expand this concept for on-chip ITP with semi-infinite sample injection (the sample is mixed in the TE reservoir) and discuss the effects of the microchannel geometry on the length (and, therefore, LoD) of analyze zones, and its effect on the total analysis time. Details on the fabrication of a single channel with large cross-section variation are provided in the Materials and Instrumentation section. For simplicity, here, we assume a fully ionized species and a constant driving current; however, the derived scaling adds significant intuition to the general cases.

Consider a channel such as that in Figure 1, which consists of two sections: a loading section with a large cross-sectional area, where the analyte is focused initially, and a detection section with a small cross-sectional area, where the analyte is detected. The rate of accumulation of species A in the loading section is given by its flux into the ITP interface,

(23) Zoom carrier ampholytes technical information. Invitrogen 25-0505B 122002.

(24) Khurana, T. K.; Santiago, J. G. *Anal. Chem.* **2008**, *80*, 6300–6307.

(25) Everaerts, F. M.; Verheggen, T. P.; Mikkers, F. E. *J. Chromatogr.* **1979**, *169*, 21–38.

(26) Verheggen, T. P. E. M.; Everaerts, F. M. *J. Chromatogr., A* **1982**, *249*, 221–230.

$$\dot{N}_t = (E_{TE}\mu_A - V_{ITP})A_L c_A^0 \quad (1)$$

Here, E_{TE} denotes the electric field in the (adjusted[24]) TE region, μ_A is the electrophoretic mobility of the analyte, V_{ITP} is the ITP velocity in the loading section, A_L is the cross-sectional area of the loading section, and c_A^0 is the analyte concentration in the adjusted TE zone. The relationship between c_A^0 and the concentration of the analyte in the reservoir is given in the work of Khurana and Santiago.[24] In the adjusted TE region (where ion concentrations are locally uniform, so that contributions of diffusive flux to ionic current are negligible), we can write the relationship between the electric field (E), current (I), cross-sectional area (A), and the conductivity (σ) as simply $E = I/(A\sigma)$. Combining this with the ITP condition that $V_{ITP} = E_{TE}\mu_{TE} = E_{LE}\mu_{LE}$ and substituting the relationships into eq 1 yields

$$\dot{N}_t = \left(\frac{\mu_A}{\mu_{TE}} - 1\right)\frac{\mu_{LE}}{\sigma_{LE}}c_A^0 I \quad (2)$$

where the subscripts LE and TE respectively denote properties of the leading and trailing electrolytes. Assuming negligible electro-osmotic flow (EOF), the temporal rate is related to the spatial (local, Eulerian) rate by $\dot{N}_x = \dot{N}_t/V_{ITP}$, yielding the relation

$$\dot{N}_x = \left(\frac{\mu_A}{\mu_{TE}} - 1\right)A_L c_A^0 \quad (3)$$

$\dot{N}_x$ represents the number of ions accumulated per distance traveled by the ITP interface and has units of mol/m. Using the subscript CI to denote a property of the counterions, the plateau concentration of the analyte is then given as[10,27]

$$c_A^P = c_{LE}\left(\frac{\mu_A}{\mu_{LE}}\right)\left(\frac{\mu_{LE} - \mu_{CI}}{\mu_A - \mu_{CI}}\right) \quad (4)$$

Next, we will assume that the accumulation of analyte in the detection section is negligible, compared to its accumulation in the loading zone. This is reasonable for loading-to-detection section area ratios of a few-fold or greater, because, as shown by eq 3, the accumulation amount scales with the local channel area. Under this assumption, the total number of moles of analyte accumulated is simply given as $N = \dot{N}_x L_L$, where L_L is the length of the loading section. The length of the analyte zone in the detection section is then given by $L_A = N/(c_A^P A_D)$, where A_D is the cross-sectional area of the detection section. Combining this with eqs 3 and 4 yields an explicit, approximate expression for the length of the analyte zone,

$$L_A = \frac{\mu_{LE}}{\mu_{TE}}\left[\frac{(\mu_A - \mu_{TE})(\mu_A - \mu_{CI})}{\mu_A(\mu_{LE} - \mu_{CI})}\right]\left(\frac{c_A^0}{c_{LE}}\right)\left(\frac{A_L}{A_D}\right)L_L \quad (5)$$

As described by Khurana and Santiago,[10] the signal-to-noise ratio (SNR) associated with the detection of an analyte can be defined as $SNR_A = L_A/\delta$, where δ is the average width of fluorescent regions dispersing into each side of the analyte zone. A high SNR_A indicates an analyte zone that is long, compared to the characteristic width of its adjoining fluorescent regions. An exact expression for the width δ is not available, because it is dependent on both the mobilities of its neighboring analyte and the mobilities of the focused CAs, which are not known *a priori*. However, the analytical expression for this characteristic diffusion-limited focusing length, given by Saville et al.,[28] shows that δ is inversely proportional to the current density. Hence, at the detector site, we can expect $\delta \propto A_D/I$. Furthermore, because of the low currents used in ITP, power sources (in particular, those of portable devices) are typically voltage-limited (and not current-limited). Assuming that the resistance of the (large cross section) loading section is negligible, the maximum obtainable current is $I_{max} = V_{max}\sigma_{TE}A_D/L_D$. Substituting the latter expressions into eq 5, and using our definition of SNR_A, we have

$$SNR_A \propto V_{max}\left(\frac{A_L}{A_D}\right)\left(\frac{L_L}{L_D}\right)c_A^0 \quad (6)$$

This result shows that the analyte SNR (and, hence, the LoD of the assay) is proportional to the ratios of cross sections between the loading section and the detection section, as well as proportional to the ratio of their lengths. Importantly, these geometrical parameters also effect the analysis time. The ITP velocity is inversely proportional to the cross-sectional area. Therefore, for a large cross-sectional area ratio, the time for an analyte zone to travel through the detection region can be neglected, compared to the time in the loading section. Hence, the total assay time can be approximated by the length of the loading section divided by the local ITP velocity, L_L/V_{ITP}. Using the expression for the maximum current, we obtain

$$t_{detect} \propto \frac{1}{V_{max}}\left(\frac{A_L}{A_D}\right)L_L L_D \quad (7)$$

Thus, the larger the cross-sectional area ratio and the larger the length of the channel section, the longer the analysis time. Clearly, there is a tradeoff between the analyte SNR (and LoD) and analysis time. Full optimization of the channel geometry is beyond the scope of this work. However, as described in the Materials and Instrumentation section, we used this result to design a microfluidic chip with a cross-sectional area ratio of 17, to compensate for the limited voltage available in our handheld device (200 V), while maintaining a reasonable analysis time of ~10 min.

EXPERIMENTAL SECTION

Carrier Ampholytes Tagging. We used two mixtures of carrier ampholyte with different isoelectric point ranges: ZOOM 3−10 and ZOOM 9−11, both obtained from Invitrogen (Carlsbad, CA). Each of the mixtures was individually labeled with an amine reactive dye (Alexa Fluor 647 carboxylic acid succinimidyl ester, also from Invitrogen (Catalog No. A-20006)).

(27) Martin, A. J. P.; Everaerts, F. M. *Proc. R. Soc. London, Ser. A: Math. Phys. Sci.* **1970**, *316*, 493–514.

(28) Saville, D. A.; Palusinski, O. A. *AIChE J.* **1986**, *32*, 207–214.

The CAs labeling protocol that we developed is adapted from the protein labeling protocol provided by Invitrogen.[29] We mixed 1 mg of Alexa Fluor 647 in 100 μL of dimethylsulfoxide (DMSO) and stored it in 10-μL aliquots at −20 °C. We prepared a stock solution of 0.2 M sodium bicarbonate (pH 8.3) obtained from J. T. Baker (Phillipsburgh, NJ). We prepared a stock solution of CAs by mixing 25 μL of ZOOM (originally 40% in aqueous solution) in 1 mL of 0.2 M sodium carbonate. This mixture was kept refrigerated at 4 °C. Finally, we prepared a stock solution of labeled CA by mixing 10 μL of ZOOM in $NaHCO_3$ with 10 μL of Alexa Fluor 647. We centrifuged the mixture for ∼10 s and incubated it at room temperature for 1 h. Assuming an average molecular weight of ∼500 Da for the CAs,[23] their final labeled concentration is ∼10 mM. The specifications for labeled CAs concentrations are given here with respect to this estimated concentration (e.g., 1-μM-labeled CAs represent a 10 000× dilution of this stock solution).

Materials and Instrumentation. For all anionic ITP experiments, the LE was composed of 10 mM lactic acid and 20 mM bis-tris (pH 6.4) in deionized water (UltraPure DNase/RNase free distilled water, GIBCO Invitrogen, Carlsbad, CA). The TE was composed of 10 mM tricine and 20 mM bis-tris (pH 7.4) in all experiments. The concentration of analytes and labeled CAs (which were mixed with the TE buffer), as well as the purity of the sample water (distilled water versus tap water), varied between experiments and are provided in the figure captions. To both the LE and TE, we added 1% ∼1MDa poly(vinylpyrrolidone) (PVP) for suppression of electro-osmotic flow (EOF).

For the experiments demonstrating the principle of the technique (see Figure 3), we used MES, ACES, and BES as ideal analytes and mixed them in the TE, together with 1 μM of labeled CAs. We diluted these analytes to their final concentration from 1 M stock solutions. This TE/sample mixture was based purely on deionized water. For the experiments demonstrating the detection of toxic chemicals, we prepared stock solutions of 1 mM 2,4,6-trichlorophenol and 10 mM 2-nitrophenol. These analytes were diluted into a TE/sample mixture that had a final composition of 50% deionized water and 50% tap water. The tap water used was from a single stock solution obtained from the city water supply at Stanford University (Stanford, CA) on May 19, 2008, with no additional preparation steps. All buffers and analytes were obtained from Sigma−Aldrich (St. Louis, MO).

We performed control and calibration experiments (and imaging), using a standard benchtop microscope or, alternatively, using a portable device. We first describe the former, which is an inverted epifluorescent microscope (IX70, Olympus, Hauppauge, NY) equipped with a 100-W mercury bulb (Ushio Inc., Tokyo, Japan), an XF100-2 filter cube from Omega Optical (Brattleboro, VT), a 10× (NA = 0.3) UPlanFl objective, and a 0.63× nonparfocalizing adapter. Images were captured using a 12-bit, 1300 × 1030 pixel array CCD camera (Micromax1300, Princeton Instruments, Trenton, NJ). We controlled the camera using Winview32 (Princeton Instruments, Trenton, NJ) and processed the images with MATLAB (R2007b, Mathworks, Inc., Natick, MA). We applied voltage using a high-voltage sourcemeter (model 2410, Keithley Instruments, Cleveland, OH). For the experiments performed on the microscope, we used off-the-shelf microfluidic borosilicate chips (model NS-95) from Caliper Life Sciences (Mountain View, CA). The channel is isotropically etched with a depth of 12 μm and consists of a 54-μm-wide section, which constricts to a 34-μm-wide section. The total length of the channel is 34.6 mm, with the initial (wide) section 11.5 mm in length. All images shown here were captured in the narrow region of the channel at a distance of 18.5 mm from the TE reservoir, 7 mm from the constriction.

Figure 2. The handheld ITP instrument (dimensions: 7.6 cm × 5.7 cm × 3.8 cm) is self-contained and includes a 5 mW laser light source, a photodiode, high-voltage generation, switching, analog-to-digital convertor, amplifier, and communication functionality. The connection in the foreground is a standard mini-USB port for both power and communication to a notebook computer. The metal casing acts as a Faraday cage to reduce environment noise.

For the data of Figure 6, we applied the FCA technique to the detection of 2NP and TCP in our portable device.[15] The device (Figure 2) is a handheld electrophoresis instrument with laser-induced fluorescence detection, which includes a microfluidic chip, high-voltage generation, switching, illumination, detection, and central processing. It is powered and controlled via USB connection to a notebook computer. Central to the handheld device is a single microelectronic chip (total silicon area of ∼4 mm × 4.5 mm and power consumption of 28 mW).[13] In its current implementation, the device is capable of sourcing up to 200 V. The experiments on the device were performed using custom borofloat microfluidic chips that we designed and built. The chip dimensions are 1.5 cm × 2.0 cm, and similar to the Caliper chip, it has a variable cross-sectional area. However, instead of varying the mask width, we used a two-etch mask process, wherein we varied the etch time of the two channel segments. The large cross section is 55 μm wide, 25 μm deep, and 11 mm long. The small cross section is 15 μm wide, 5 μm deep, and 17 mm long. The variable etching time affects both the width and the depth of the channel and results in a 17:1 cross-sectional ratio, versus the 2.4:1 ratio in the Caliper chip. The detector was located at a distance of 20 mm from the TE reservoir (9 mm from the channel constriction).

Assay Protocol. Figures 1S and 2S in the Supporting Information document show, respectively, the geometry of the custom-made chip and a schematic of the ITP injection protocol (applicable to both chip geometries). Briefly, we filled reservoirs number 2, 3, and 4 with LE by applying a vacuum to reservoir 1 until all channels were filled. We then rinsed reservoir 1 (using a syringe)

(29) Invitrogen, Amine-Reactive Probes, Publication MP 00143, 2007.

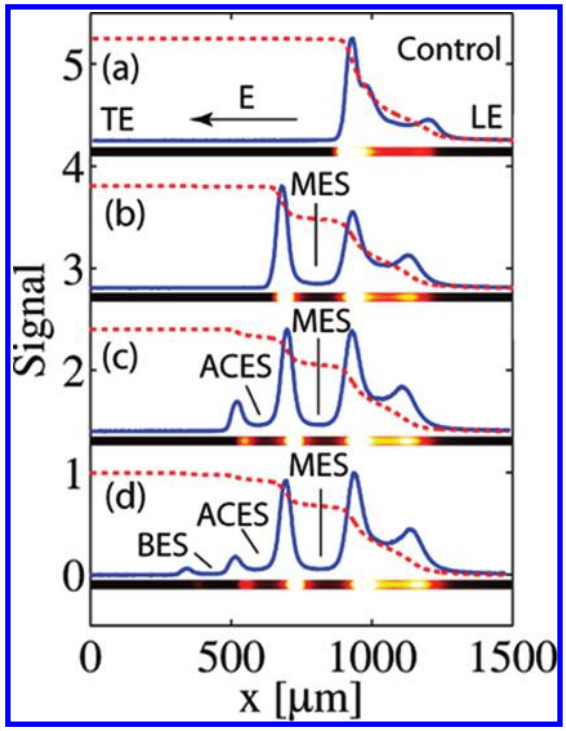

Figure 3. Demonstration of the FCA assay under controlled conditions (in an epifluorescence microscope), using Good's buffers as idealized analytes: (a) The control case shows the distribution of fluorescent CAs in the "ultrapure" water sample; (b) 10 μM of MES is mixed with the TE and creates a zone between the LE and TE (the zone displaces labeled CAs, resulting in a new gap in the signal). (c, d) 10 μM each of ACES and BES are sequentially added, further displacing the labeled CAs and resulting in additional gaps in the signal. All signals and images are normalized by their maximum value. Solid curves show the fluorescent signal averaged across the cross-sectional area of the channel, as recorded in the experiment. Raw intensity images of the fluorescent peaks are presented under each signal. Also shown (dashed line) are LE-to-TE integrals of the CA signal. LE is 10 mM lactic acid, TE is 10 mM tricine, and the counterion is 20 mM bis-tris. We mixed 1 μM of ZOOM 3−10 labeled with Alexa Fluor 647 in the TE. The process was performed at a constant current of 0.2 μA, with an exposure time of 100 ms. The time elapsed from initiation of the voltage to arrival of the analytes to the detector is ~120 s.

several times with distilled water and filled it with the TE, analytes, and a labeled mixture of CAs. The electrodes were placed in reservoirs 1 and 4, and either a constant voltage or current was applied (values listed in the figure caption of Figure 2S).

RESULTS AND DISCUSSION

Principles and Demonstration of the Technique Using a Standard Microscope. Figure 3 shows calibration and control experiments for the FCA technique. Here, we use several (well-known, well-characterized) Good's buffers as idealized analytes. In the negative control (Figure 3a), no analytes are present and a large subset of the labeled CAs with effective mobilities between those of the LE and TE focus at the interface. We hypothesize that the underlying distribution of the CA signal (which resembles several large, overlapping peaks) is affected by buffer impurities. Nevertheless, these impurities and the CAs form a standard baseline signal associated with this CA mixture in the absence of analytes of interest. In Figure 3b, we show the effect of adding 10 μM of MES to the TE mixture. A new plateau ITP zone is created by MES, displacing a subset of the CAs. The displacement results in a new gap in the fluorescence signal (whose width is directly proportional to its initial concentration, as described by Khurana and Santiago).[10] In other words, FCAs with respectively higher and lower effective mobilities are displaced by the analyte toward the LE and TE. In Figure 3c, we show the effect of a second analyte, ACES, mixed with the TE. The ACES zone causes a new gap in the signal. The intensity of the fluorescent peak trailing the MES zone has decreased, as part of the CAs were displaced to a new location (trailing the ACES zone). Figure 3d shows similar displacement with the addition of BES. Note the reproducibility of the signal shape away from analyte zones. For example, note the width and relatively location of the peaks to the left of the MES in all four experiments. Signal analysis and interpretation of the results benefit from this repeatability.

The data of Figure 3d shows that the number of CAs with mobilities lower than BES (to the left in the figure) is small, compared to the total number of CAs. This results in a low-area local peak on the trailing end of the CA signal and suggests that the carrier CA mixture used here (ZOOM 3−10) has fewer species with pK_a values sufficiently high to yield low effective mobilities, relative to BES. (See Righetti et al.[19] for a discussion on the content and pK_a values of several commercial CA mixtures.) Below, we will discuss the redistribution of CA signals using CAs of mixtures designed for a different pH range.

The dashed line in Figure 3c shows an integral of the CA fluorescence intensity curve. This integral curve can be used to extract information about the effective mobilities of the analytes, thus assisting in identification. Integration of the signal may also help make the analysis more robust to noise. We explore such signal analysis in a separate publication[30] and focus here on other properties of the technique and its implementation on a handheld device. Figure 3S in the Supporting Information document presents a similar detection sequence for cationic ITP, where the CAs are labeled with carboxyrhodamine 6G.

Detection of 2,4,6-Trichlorophenol in Tap Water Using a Microscope. Figure 4 presents quantitative detection of TCP in tap water, without additional sample preparation steps. We spiked tap water with a range of TCP concentrations and mixed it with the TE and labeled CAs, resulting in a 2-fold dilution of the sample. We then applied ITP directly to that sample. As in the previous example, subsets of labeled CAs are displaced by and bracket the TCP zone. The width of the gap in the signal (analyte zone width) is proportional to the initial concentration of the analyte, as per eq 5. Similar relationships between the widths of the analyte zones and the initial concentration in indirect detection ITP assays were discussed and have been shown by Khurana and Santiago[10] and Chambers and Santiago.[9] The LoD is reached when the local minimum of the signal can no longer be resolved relative to normal, local fluctuations. Figure 4b shows the minimum concentration for which a new minima in the signal is discernible with confidence. We note that, in these experiments, we focused on illustrating the applicability of the technique to relevant water pollutants. As discussed in the Theory section, the LoD of the technique is strongly dependent on the channel geometry and buffer chemistry. Here, we have used a commercial chip and a

(30) Bercovici, M.; Kaigala, G. V.; Santiago, J. G. *Anal. Chem.* **2009**, DOI: 10.1021/ac9025658.

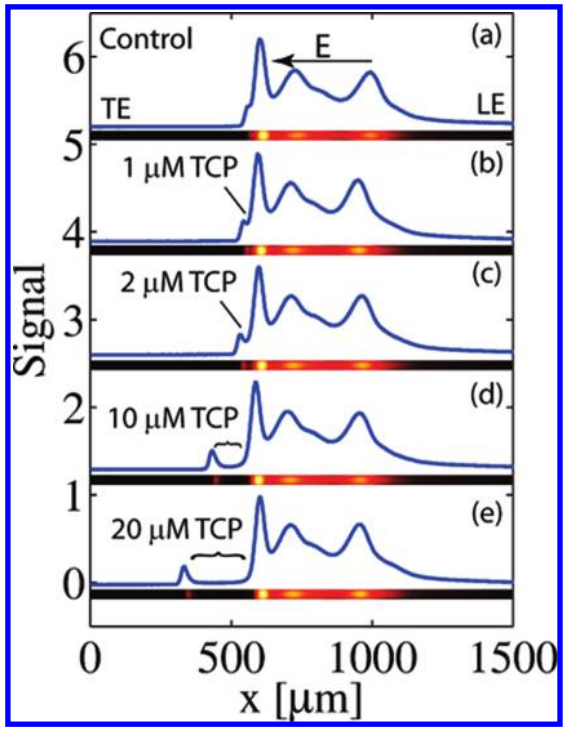

Figure 4. Indirect detection of 2,4,6-trichlorophenol (TCP) in tap water (performed on an epifluorescent microscope). (a) In the control, we observe the underlying distribution of labeled CAs, which are likely affected by impurities inherent in the water sample. We consider this as the baseline signal. (b−e) When TCP is added at a range of concentrations from 1 μM to 20 μM, we see the formation of a signal gap with SNR proportional to the initial analyte concentration. The buffers, labeled CAs, microchannel geometry, and applied current are the same as those described in Figure 3.

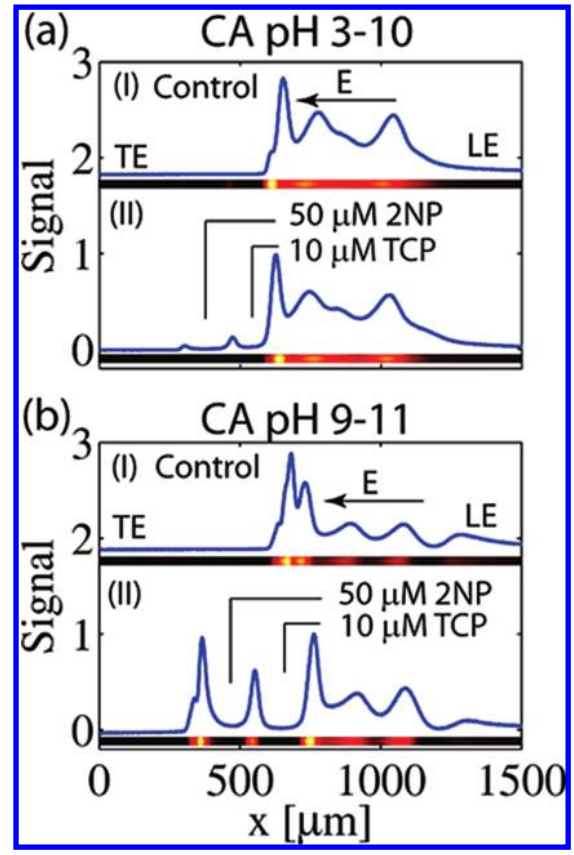

Figure 5. Detection of 2-nitrophenol (2NP) and 2,4,6-trichlorophenol (TCP) in tap water (in a microscope) using (a) CAs with a pI range of 3−10, (b) CAs with a pI range of 9−11. For both cases: (I) the control (no analytes) shows several peaks, corresponding to impurities in the tap water; and (II) 50 μM of NP and 10 μM of TCP are introduced mixed in the TE reservoir. Each displaces a subset of fluorescent CAs resulting in new gaps in the signal. At the working pH (~6.4 in the LE, ~7.4 in the TE), the pI 9−11 CA mixture provides a larger number of low (effective) mobility CAs and, thus, contribute to the area and magnitude of the peaks bracketing the analytes. Experiments performed on an epifluorescent microscope. Raw inverted-intensity images of the fluorescent peaks are shown under each signal. LE and TE are the same as in Figure 3. We here used an applied voltage of 1100 V with an exposure of 2 ms. The time elapsed from the initiation of the voltage to the arrival of the analytes to the detector is ~60 s.

high-concentration TE buffer: these are two controlling variables that could be significantly improved to achieve lower LoD. We estimate that the current LoD of the FCA technique is ~1 μM for most analytes (e.g., see the data in Figure 4). In future work, we will further improve the LoD.

Redistribution of CA Signal and Detection of Multiple Toxins in Tap Water. The FCA technique allows for detection of multiple analytes present in the sample. In this section, we apply the technique for the detection of 2NP and TCP in tap water. We also use this example to illustrate how the associated distribution of CAs, relative to analytes, can be modified to change the range of detectable analyte mobilities and SNR values.

Figure 5a presents an experiment where 2NP and TCP are both detected in tap water. We first note the underlying baseline of the CAs, which resembled several overlapping peaks. In these experiments, we used labeled CAs with a pI range of 3−10 (the broadest range commercially available from most vendors). While the CA zones bracketing TCP and 2NP are clearly visible, the area under the curve of CAs, which are on the TE side of the 2NP zone, is low (reflecting a low number of CAs with effective mobilities lower than those of 2NP).

One possible approach to improve the signal in the case above is to choose a counterion with a higher pK_a value, thus increasing the pH of the entire system and increasing the effective mobilities of the two analytes. Depending on the (unknown) pK_a values of the CAs, this may result in the analytes displacing a larger number of CAs and increasing the signal. However, this approach carries the inherent disadvantage that increasing the pH of the system also increases the effective mobility of the TE. Because the focusing rate is proportional to the ratio of analyte to TE mobilities (eq 3), this will lead to shorter analyte zones and will adversely impact the limit of detection. An alternative approach is to use a different mixture of CAs, which, for a given pH, is expected to include a larger number of low-effective-mobility CAs. CAs with higher isoelectric points are also expected to have higher pK_a values and, therefore, lower (anionic) effective mobilities. In Figure 5b, we present a second experiment, identical to that of Figure 5a, except, here, we use labeled CAs with a pI range of 9−11 (highest range commercially available). As expected, these CAs have lower effective mobilities and a larger fraction of them focus between the analytes and the TE. This results in more confidence associated with the identification of the signal gap (e.g., here the signal-to-noise ratio of the

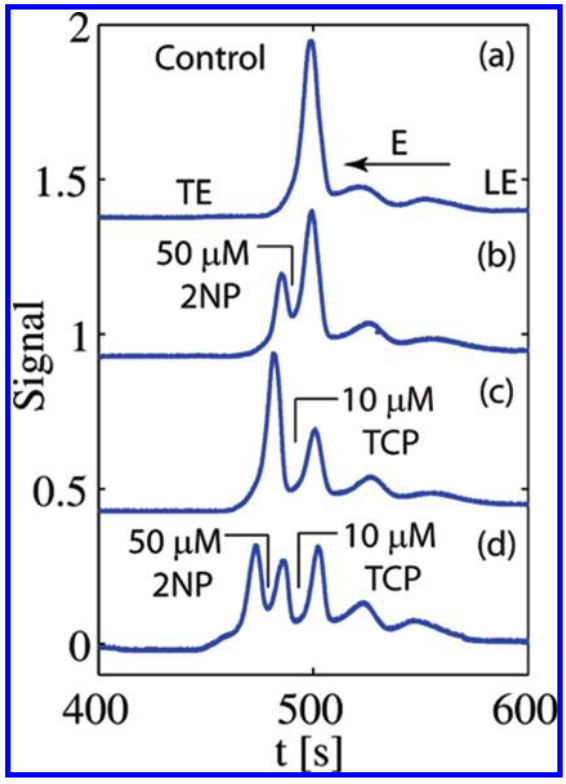

Figure 6. Detection of unlabeled 2NP and TCP in tap water using the handheld ITP device shown in Figure 2. LE and TE compositions are the same as those in Figure 5. A potential of 200 V was applied along a 23-mm channel with a cross-sectional area variation of 17:1 (the detection region is 17 mm long). Despite less available voltage and longer analysis time, the handheld device successfully detects both toxins.

peak of slower CAs is ~20-fold higher than that in Figure 5a). This enrichment process in which the fluorescence intensity of signal peaks can be redistributed is especially important for implementation on miniaturized and low-cost devices, where, often, the dynamic range and sensitivity of the sensor may be low, compared to benchtop, microscope-based systems.

Implementation of the Fluorescent Carrier Ampholyte Assay for Toxins Detection in a Handheld Device. Lastly, we integrate the analyses and experience associated with the theory and empirical, detailed imaging analysis to demonstrate the detection of unlabeled toxins (2NP and TCP) in untreated tap water in our portable device (c.f. Materials and Instrumentation above). Figure 6 presents the detection of 2NP and TCP in tap water, using the same buffer chemistry used previously. We used the same CAs (pI range of 9−11) as those in Figure 5b; however, here, we implemented the assay in our handheld device rather than a standard microscope system. The most significant differences between the handheld device and the benchtop system are the lower spatial resolution of the detector, and the associated limit on high voltage (the handheld device is currently limited to 200 V). Both limitations result in wider (more-diffused) gradients in the CA signals (larger values of δ in eq 6) and, therefore, reduce the LoD. To provide some compensation for these limitations, we designed microfluidic channels with a high cross-sectional area ratio (17:1). As shown by eq 5, a higher area ratio implies proportionally longer analyte zones in the detection section. Furthermore, as the zone enters the detection section, the current density increases 17-fold, resulting in sharper ITP interfaces (smaller δ values). Both parameters contribute to an increase in the SNR associated with analyte detection (as per eq 6).

In Figure 6, we show the detection of 2NP and TCP at concentrations equal to those in the microscope-based experiments presented earlier. Note that some finer features of the signal have been lost to the lower resolution of the detector. Furthermore, as indicated by eq 7, although a large area ratio improves the resolution of the assay, it also increases the total analysis time. As indicated by the (temporal) isotachophorerogram, the total analysis time on the handheld device was ~10 min. Clearly, there is a tradeoff between resolution and analysis time, which is a strong function of maximum voltage, channel geometry (both length and area ratios), and buffer chemistry. In this work, we were primarily focused on a proof of concept for detection on a handheld device and, therefore, did not further optimize system sensitivity. We will pursue optimizations of both sensitivity and mobility resolution in future work.

CONCLUSIONS

We developed a novel indirect-detection technique that allows the detection of analytes with little *a priori* knowledge of their electrophoretic mobilities. The technique is based on the displacement of fluorescently labeled carrier ampholytes by focused analytes in ITP. The gaps in the resulting fluorescence signal are used to detect the analytes indirectly. We have demonstrated the detection of ideal analytes and of 2-nitrophenol (2NP) and 2,4,6-trichlorophenol (TCP) in tap water, without the need for labeling or sample preparation. We presented experimental demonstrations using both a standard microscopy-based system and a handheld device. The signal produced by the FCA assay can be easily detected using the highly simplified optics on our handheld device. This opens the possibility for portable and low-cost detection systems for toxins in the environment.

Our current LoD is ~1 μM for most addressable analytes. This level of sensitivity is relevant for some pollutants such as 2-chlorophenol, 2,4-dichlorophenol, and 2,4-dimethylphenol, which are permitted by the EPA at levels of ~1 μM.[31] However, further improvements are required to achieve limits of detection on the order of 10 nM or better, which are necessary to meet EPA standards of other toxins such as 2NP and TCP.[31] We believe that such sensitivity is possible with the current technique, and, therefore, it can eventually become competitive with the sensitivity of high-quality, existing (benchtop) chromatography techniques. We are currently exploring several directions to achieve this. First, we hypothesize that significant improvements in LoD are possible by optimizing the microchip geometry, particularly by increasing the cross-sectional area ratio. On the microscope system, a 50:1 ratio (versus a ratio of 2.4:1 in the off-the-shelf chip) should theoretically allow for ~50 nM detection. On the handheld device, chip geometry optimization should be performed in concert with efforts to increase system voltage to maintain a suitably short analysis time. In addition, by applying an LE concentration cascade,[32] we believe that an additional 10× increase in sensitivity is possible. Optimization of the TE chemistry should also help.

(31) National Recommended Water Quality Criteria, U.S. Environmental Protection Agency, http://epa.gov/waterscience/criteria/wqctable/, 2009.
(32) Bocek, P.; Deml, M.; Janák, J. *J. Chromatogr., A* **1978**, *156*, 323–326.

For example, reducing the TE concentration and TE mobility (e.g., by choosing a TE with a higher pK_a value) would proportionally increase the focusing rate. We believe that an additional factor of ~10 or more is possible with these improvements. Other possibilities for improved LoD include off-chip sample treatments for sample purification (as is often used with other systems).

In a separate publication,[30] we present a signal analysis technique that enables analyte identification based on the fluorescent signal. As we have shown here, the higher the effective mobility of the analyte, the larger fraction of labeled CAs that it displaces. Quantifying this fraction can be used to measure an analyte's effective mobility. Measurements of the effective mobility under different pH conditions allows one to extract the pK_a value and fully ionized mobility of the analyte, which assist in identification.

ACKNOWLEDGMENT

M.B. is supported by an Office of Technology Licensing Stanford Graduate Fellowship and a Fulbright Fellowship. G.V.K. is supported by a postdoctoral fellowship from the Natural Science and Engineering Research Council of Canada. We thank Mr. Takashi Matsumura from Ebara Corporation, Japan, for advice on labelling protocols, insightful discussions, and constructive comments. We gratefully acknowledge support from the Micro/Nano Fluidics Fundamentals Focus (MF3) Center funded by Defense Advanced Research Projects Agency (DARPA) (MTO Grant No. HR0011-06-1-0050) and contributions from MF3 corporate members. We also gratefully acknowledge the support of the Defense Advanced Research Projects Agency (Contract No. N66001-09-1-2007) (Dr. Dennis Polla, program manager).

SUPPORTING INFORMATION AVAILABLE

Further details on the geometry of the custom-made chip that we used in the detection of 2-nitrophenol and 2,4,6-trichlorophenol on our handheld device is provided in figure S1. The injection protocol is detailed in figure S2. Figure S3 shows an example where the fluorescent carrier ampholytes assay is used for detection of analytes in cationic isotachophoresis. (PDF) This material is available free of charge via the Internet at http://pubs.acs.org.

Received for review November 5, 2009. Accepted January 11, 2010.

AC902526G